American Mineralogist, Volume 68, pages 315–333, 1983

Petrogenesis of the Concord gabbro–syenite complex, North Carolina

BARBARA A. OLSEN[1], HARRY Y. MCSWEEN, JR.

Department of Geological Sciences
University of Tennessee
Knoxville, Tennessee 37996

AND THOMAS W. SANDO

Department of Earth and Planetary Sciences
Massachusetts Institute of Technology
Cambridge, Massachusetts 02139

Abstract

The Concord intrusive complex, Cabarrus County, North Carolina, consists of a large gabbro stock enveloped by a horseshoe-shaped syenite ring dike. The complex is clearly delineated from surrounding rocks by magnetic and radioactivity anomalies. Gravity modeling suggests that the gabbro pluton extends to a depth of about 6 km and that the syenite ring dike dips steeply outward at an angle of 78° on the west side and dips vertically on the east side. A Sm–Nd mineral isochron for gabbro and a Rb–Sr isochron for syenite indicate that the two lithologies were emplaced contemporaneously ~405 m.y. ago. Initial Nd and Sr isotopic compositions of gabbro and syenite in this complex overlap, suggesting the two rock types may be related through closed-system fractional crystallization.

Three gabbroic rock types are distinguished, based on the presence of different cumulus minerals: olivine–plagioclase, olivine–clinopyroxene–plagioclase, and clinopyroxene–plagioclase. Some magnetite and ilmenite occur as inclusions in these early phases and are probably cumulus as well. All gabbros contain postcumulus orthopyroxene and hornblende (±clinopyroxene), as well as minor biotite, sulfides, and apatite. The syenite is a seriate porphyry with megacrysts of perthitic feldspar in a groundmass of albite, microcline, clinopyroxene, amphibole, biotite, quartz, Fe–Ti oxides, pyrite, apatite, zircon and monazite. Mafic mineral compositions in gabbro and syenite indicate that fractionation involved only limited Fe-enrichment.

Geochemical modeling of major and trace element variations indicates that the Concord syenite could have been produced by fractionation of olivine, plagioclase, clinopyroxene, and minor Fe–Ti oxide minerals, of the same compositions as observed cumulus phases in the Concord gabbro, from a basaltic parental magma similar in composition to the Concord gabbro. This gabbro–syenite trend probably represents differentiation of a tholeiitic basaltic melt near a thermal divide along the critical plane of silica undersaturation. This fractionation took place in a magma reservoir at depth, before intrusion of the syenitic residual liquid into the fractured region between previously intruded gabbro and country rock.

Introduction

The Concord intrusive complex in Cabarrus County, North Carolina, offers the best exposure of the gabbro–syenite association in the southern Appalachian Piedmont, among the several examples previously described from this region (Medlin, 1968; Wilson, 1981). This complex consists of a large gabbro pluton partially enclosed by a ring dike of syenite. This paper will demonstrate that these intrusive bodies are related temporally as well as spatially. It has been inferred previously (*e.g.*, Butler and Ragland, 1969) that the syenite is a later differentiate of the same parental magma that produced the gabbro; this study substantiates that idea using petrologic observations, chemical models, and isotopic constraints.

The Concord intrusive complex has been a focus of geologic interest for many years. The rocks of the Con-

[1] Present address: Gulf Oil Exploration and Production Company, Bakersfield, California 93302.

0003–004X/83/0304–0315$02.00

cord area were first described by Watson and Laney (1906) in a report on the ornamental and building stones of Cabarrus and Mecklenburg counties. Preliminary geologic maps of the Concord complex were prepared by White and Mundorff (1944), LeGrand and Mundorff (1952), and Bell (1960); the latter study also described the economic potential of the area. Airborne magnetic and radioactivity surveys of the Concord area were conducted by Johnson and Bates (1960), and Morgan and Mann (1964) reported a detailed gravity study of the area. Bulk chemical analyses of Concord gabbro samples were given by Cabaup (1969), and average analyses of gabbro and of syenite were reported by Butler and Ragland (1969). Price (1969) analyzed trace elements in both gabbro and syenite samples. The crystallization age of the Concord syenite was measured by Fullagar (1971). These geophysical and geochemical studies will be reinterpreted in light of new field, petrologic, and geochemical data presented here.

Analytical techniques and sources of data

Thin sections of Concord gabbro (1000 points) and syenite (500 points) were point-counted for modal analyses. In order to distinguish plagioclase from alkali feldspar, the syenite thin sections were stained with sodium cobaltinitrate solution. Modal percentages are reported in Table 1. The minimum error of the modal determinations ranges from 1–10% relative using the chart of Van der Plas and Tobi (1965); actual analytical error may be greater due to relationships between adjacent grains and to layering (Neilson and Brockman, 1977).

Mineral compositions were determined using an automated MAC 400S electron microprobe at the University of Tennessee, utilizing the correction procedures of Bence and Albee (1968) and the data of Albee and Ray (1970). Analyses using a slightly defocussed electron beam (~5–15 μm diameter) were performed on minerals in 9 polished thin sections. Operating conditions were set at 15 kV and 0.03–0.05 μa beam current, depending on the mineral to be analyzed. For amphibole analyses Fe^{3+} was calculated using the method of Leake (1978), and for oxide analyses Fe^{3+} was calculated based on stoichiometry. Representative analyses of major minerals are presented in Table 2; a complete compilation of microprobe analyses can be found in Olsen (1982).

Bulk chemical analyses for major elements in 40 Concord gabbro samples were obtained from an unpublished thesis by Cabaup (1969). Butler and Ragland (personal communication, 1980) supplied individual bulk chemical analyses for major elements for 7 Concord syenite samples and 6 Concord gabbro samples (previously published in summary form by Butler and Ragland, 1969), and chemical analyses for trace elments on the same samples were taken from an unpublished dissertation by Price (1969). All bulk analyses reported total Fe as Fe^{2+}; for normative calculations $Fe_2O_3/(FeO+Fe_2O_3)$ ratios for average gabbro (0.24) and average syenite (0.45) taken from Nockolds (1954) were used to correct the Fe values in the analyses.

One fresh sample of gabbro containing abundant clinopyroxene (CFG–5 in Table 1) was selected for age-dating by the Sm–Nd mineral–isochron method. After crushing and sieving to obtain a 25–100 ϕ size fraction, crude separation of plagioclase and pyroxene was effected using a Frantz magnetic mineral separator. 130 mg of pyroxene and 240 mg of plagioclase were hand-picked from these separates for analysis. Only clean, inclusion-free plagioclase was accepted. Some opaques were unavoidably included in the clinopyroxene fraction due to the intimate intergrowth of these two minerals, but material containing inclusions of any other mineral was avoided. After washing in 2.5 N HCl for one hour the separates were dissolved in an ultra-pure $HF–HNO_3–HClO_4$ mixture, and a split of the dissolved material was spiked for isotope-dilution determination of Sm and Nd concentrations. 100 mg each of powdered whole-rock gabbro CG–5 and syenite CS-0 were also dissolved for analysis. Separation of Sm and Nd followed a two-column cation-exchange technique described by Zindler *et al.* (1979). Analyses were performed on the 9-inch automated mass spectrometer at the Massachusetts Institute of Technology. Nd isotopic composition measurements were made on the unspiked fraction of samples. Procedural blanks for this method are less than 0.1 ng for both elements, and no blank corrections were required for any of the measurements. Analytical precisions as judged by replicate analyses of standards are 0.5% for Sm/Nd ratios and 0.003–0.004% for $^{143}Nd/^{144}Nd$. Values of $^{143}Nd/^{144}Nd$ reported here are relative to 0.512630 for U.S.G.S. standard rock BCR-1.

Field relationships

The Concord intrusive complex occurs within the Charlotte belt of the southeastern Piedmont. The rocks of the Charlotte belt have experienced Paleozoic regional metamorphism of greenschist to amphibolite facies grade and are intruded by a bimodal suite of gabbroic and granitic plutons. According to Bell (1960), the Concord pluton is surrounded by "massive and foliated dioritic and mafic rocks", with "granitic and granodioritic gneisses" in contact with the syenite body on the east and west. Outcrops of country rocks near the complex are extremely scarce, but observations of saprolite indicate Bell's map units to be generally correct.

The Concord complex consists of a discontinuous syenite ring dike with varying thickness that partially encircles a gabbro body of roughly oval shape. Both lithologies are cut by numerous small pegmatite and less abundant diabase dikes. Field mapping of the Concord area was carried out using portions of the Concord, Southeast Concord, Kannapolis, and Harrisburg Quadrangle U.S.G.S. 1:24,000 scale topographic maps. Figure 1 is a geologic map based on this work and modified from

Table 1. Modal variations (volume %)

	Concord Gabbro											
	Plg	Hbl	Bio	Opq	Cpx	Opx	Olv	Apa	Serp	Chl	Ser	Zir
CG-4	64.1	5.5	0.4	1.4	16.1	10.9	-	0.7	0.4	0.3	0.2	-
CG-5	56.8	2.5	4.6	6.9	15.8	12.1	-	0.4	0.1	0.7	0.1	-
CG-6	69.5	7.1	0.6	2.7	5.5	7.9	5.0	0.2	0.4	0.7	0.3	0.1
CG-9	52.1	24.7	0.9	5.9	0.7	10.3	2.7	0.6	-	1.9	0.2	-
CG-10a	51.3	29.6	-	2.2	5.1	7.2	3.0	-	-	0.9	0.7	-
CG-10b	46.9	26.3	-	1.1	18.5	5.8	-	0.4	0.4	0.2	0.4	-
CG-11	61.6	5.0	-	4.3	12.8	14.0	1.0	0.3	0.3	0.6	0.1	-
CG-22	45.2	36.6	-	6.5	0.6	4.5	0.1	0.7	0.1	2.8	2.9	-
CG-23	52.1	30.3	0.1	2.5	3.0	8.8	0.9	0.4	-	1.8	-	0.1
CG-25	57.3	24.1	0.2	3.0	1.8	9.6	3.0	0.3	0.1	0.3	0.3	-
CG-26	47.2	33.3	0.1	3.3	2.7	10.8	1.5	-	-	0.5	0.6	-
CG-27	58.9	11.7	-	1.9	0.1	13.8	12.4	0.3	0.2	0.2	0.5	-
CG-33	59.3	20.2	3.1	2.4	2.2	9.1	1.7	-	0.2	1.6	0.2	-
CG-47	46.2	36.8	0.4	3.2	0.7	11.8	-	0.2	-	0.4	0.3	-
CG-50	68.9	4.0	-	2.3	3.0	3.6	16.1	0.1	0.5	0.5	1.0	-
CG-53	62.8	5.6	1.5	2.2	2.9	10.5	13.4	0.2	0.4	0.1	0.4	-
CG-54	47.5	16.7	1.6	4.5	2.6	11.4	14.6	0.2	-	0.4	0.5	-
CG-57	65.3	8.0	2.3	3.5	0.8	12.8	6.2	0.3	-	0.5	0.3	-
CG-58	65.8	3.7	1.3	3.2	12.9	7.4	4.9	-	0.1	0.5	0.2	-
CG-73	62.4	1.9	1.7	4.0	14.2	7.2	7.4	-	0.1	0.2	0.9	-
CG-74	64.9	7.3	3.1	5.6	10.2	6.9	0.9	0.2	0.4	0.3	0.2	-
CG-81	58.5	7.9	4.0	5.2	12.2	11.8	-	0.3	-	0.1	-	-
CG-84	65.5	3.4	-	5.5	6.0	15.3	3.5	0.3	0.1	0.3	-	0.1
CG-87	64.5	14.7	-	4.4	1.0	10.8	2.7	0.1	0.2	0.8	0.6	0.2
CG-90	64.5	10.4	1.6	2.8	0.2	13.7	5.1	0.2	-	1.2	0.3	-
CG-92	62.2	15.8	1.5	2.7	6.6	7.7	2.9	-	-	0.4	0.2	-
CG-98	58.4	4.2	-	8.2	10.8	11.2	6.4	-	0.4	0.4	-	-
CG-102	50.6	17.6	-	3.5	12.2	10.7	4.7	-	0.1	0.3	0.3	-
CG-104	53.0	25.8	2.0	2.4	0.4	15.0	0.4	0.3	0.5	-	0.2	-
CG-105	51.0	21.3	-	2.3	8.9	15.7	-	0.3	-	0.4	0.1	-
CG-106a	53.9	16.2	-	3.9	14.9	10.5	-	0.4	-	0.1	0.1	-
CG-106b	54.3	24.4	-	5.2	4.7	10.5	-	0.4	-	0.5	-	-
CG-107	51.8	23.7	-	6.5	17.7	8.9	-	0.2	0.1	0.6	0.5	-

	Concord Syenite										
	Plg	Hbl	Bio	Opq	Cpx	Ksp	Prth	Qtz	Mon	Apa	Zir
CS-39	4.3	1.3	0.2	2.6	2.6	3.4	82.4	2.6	0.6	-	-
CS-62	4.8	3.1	0.2	2.9	4.2	3.1	77.0	4.0	0.4	0.4	-
CS-88	3.2	-	-	-	-	3.2	57.0	36.1	-	-	0.4
CS-2	0.5	0.4	0.4	2.9	5.1	0.5	86.6	0.7	1.1	0.9	0.9
CS-37	18.6	-	1.8	1.8	2.7	1.8	68.5	3.9	0.4	0.6	-
CS-20a	4.8	1.0	0.6	3.0	4.2	1.5	79.8	3.2	1.0	0.8	0.2

Bell (1960), White and Mundorff (1944), and LeGrand and Mundorff (1952). The latter maps, which show the syenite body to be continuous at the surface across the northern end of the pluton, are in disagreement with the map of Bell (1960), which denotes a parentheses shape for the syenite body, open at the northern and southern ends. Syenite outcrops and quarries occur at the nothern end, confirming the horseshoe shape described earlier by White and Mundorff (1944).

The Concord gabbro is exposed as large, spheroidally weathered, black boulders. The syenite occurs mainly as pedestal-shaped boulders, and quarries provide abundant fresh samples. The syenite outcrops are much larger than the gabbro boulders and are more highly weathered. Due to the paucity of outcrops, lithologic contacts have not been observed, but can be fixed rather closely because the syenite forms a distinct topographically high area (~100 ft. in relief) relative to gabbro and country rocks. These two units can also be recognized from saprolite: the gabbro forms dark gray soils of the Mecklenburg and Iredell soil series, whereas light-colored arkosic soil is produced from weathering of syenite. There is additional geophysical evidence which is useful in determining the location of contacts at the surface, as well as suggesting the geometry of the pluton at depth.

Geophysical expression

The results of two geophysical studies conducted in the Concord area are available for comparison with the mapped outcrop pattern of the complex. The first is an aeromagnetic and aeroradioactivity survey of the Concord quadrangle by Johnson and Bates (1960). On their magnetic map, a group of closely-spaced contours coincides with the inner boundaries of the syenite body. The cause of the 4500 gamma anomaly that surrounds the gabbro is not clear, though Johnson and Bates suggested that magnetite might be concentrated along the contacts between the gabbro and syenite. Three smaller gabbro bodies extending out from the southern end of the pluton, the northernmost of which is shown in Figure 1, also coincide with magnetic anomaly patterns. Johnson and Bates' radioactivity map shows the syenite body outlined by two parenthesis-shaped areas of high radioactivity on the eastern and western margins. This feature undoubtedly influenced Bell's (1960) interpretation of the syenite outcrop pattern, and may suggest that the syenite to the north of the Concord gabbro is much thinner.

The second geophysical report is a detailed gravity study of the Concord Quadrangle by Morgan and Mann (1964). This work included calculations of Bouguer anomalies, which were displayed on maps showing the simple Bouguer anomaly and the residual anomaly; appropriate portions of both maps are shown in Figure 2. On the simple Bouguer anomaly map (Fig. 2a), the gabbro intrusion shows a pronounced increase in Bouguer value, reaching a maximum of +35.5 milligals in the center. The simple Bouguer anomaly map reflects large-scale regional trends and deep-seated mass distributions and can be

Table 2. Representative microprobe analyses of minerals

	Gabbro Clinopyroxene		Syenite Clinopyroxene		Gabbro Orthopyroxene		Gabbro Olivine	
	CG-10[5]	CG-50[6]	CS-12[5]	CS-51[5]	CG-33[7]	CG-9[8]	CG-9[8]	CG-73[4]
SiO_2	51.3(6)	51.3(12)	53.1(4)	53.7(4)	53.8(4)	54.4(4)	37.4(2)	37.8(4)
TiO_2	0.59(5)	1.03(32)	0.59(23)	0.21(2)	0.08(2)	0.12(2)	-	-
Al_2O_3	2.29(20)	3.76(60)	1.36(11)	0.64(6)	1.38(7)	1.49(9)	-	-
FeO	8.51(26)	6.71(62)	8.70(35)	10.4(2)	16.4(1)	15.6(2)	26.5(2)	23.6(1)
MnO	0.37(4)	0.14(1)	1.32(2)	1.87(13)	0.48(2)	0.41(3)	0.50(4)	0.57(3)
MgO	15.0(2)	15.6(4)	15.1(3)	12.2(2)	26.5(3)	27.6(2)	35.4(3)	38.1(2)
CaO	21.1(2)	21.3(7)	19.4(2)	19.8(1)	1.00(9)	0.82(13)	-	-
Na_2O	0.50(2)	0.52(11)	0.69(3)	1.43(6)	0.03(1)	0.03(2)	-	-
Total	99.72	100.36	100.26	100.20	99.72	100.38	99.80	100.07
Cation Basis (O)	6	6	6	6	6	6	4	4
Si	1.917	1.888	1.969	2.013	1.958	1.953	0.996	0.989
Ti	0.016	0.028	0.016	0.005	0.002	0.003	-	-
Al	0.100	0.163	0.059	0.027	0.059	0.062	-	-
Fe	0.265	0.206	0.269	0.326	0.500	0.467	0.591	0.516
Mn	0.011	0.003	0.041	0.059	0.014	0.011	0.011	0.012
Mg	0.833	0.854	0.832	0.681	1.437	1.475	1.404	1.489
Ca	0.845	0.839	0.770	0.794	0.038	0.030	-	-
Na	0.035	0.037	0.049	0.103	0.002	0.002	-	-

Table 2 (continued)

	Gabbro Amphibole		Gabbro Amphibole		Gabbro Biotite		Syenite Biotite	
	CG-50[3]	CG-73[4]	CS-43[6]	CS-51[5]	CG-5[4]	CG-73[4]	CS-51[5]	CS-12[5]
SiO_2	41.6(2)	41.5(2)	49.6(6)	50.8(4)	37.4(22)	37.6(6)	40.4(8)	38.9(12)
TiO_2	3.15(10)	4.04(11)	1.28(17)	0.92(6)	6.84(22)	3.76(38)	2.10(23)	5.11(14)
Al_2O_3	11.9(2)	11.9(1)	3.93(7)	3.09(2)	14.1(2)	16.4(9)	11.5(4)	12.8(4)
$*Fe_2O_3$	4.70	1.70	10.3	9.34	-	-	-	-
FeO	4.95(26)	9.63(29)	3.58(29)	3.15(11)	11.4(2)	7.90(60)	12.9(6)	14.3(2)
MnO	0.18(3)	0.21(2)	1.50(10)	1.76(7)	0.05(4)	0.00	0.61(9)	0.35(4)
MgO	15.6(3)	13.3(1)	16.1(3)	16.7(2)	15.5(3)	19.2(10)	18.1(4)	16.0(3)
CaO	11.8(2)	11.5(1)	10.3(4)	9.84(14)	-	-	-	-
Na_2O	2.64(10)	2.41(11)	1.93(16)	2.41(10)	0.20(4)	0.59(16)	0.09(1)	0.14(3)
K_2O	0.84(1)	1.13(5)	0.56(4)	0.67(2)	9.55(7)	8.73(74)	9.12(24)	9.05(35)
Total	97.29	97.24	99.12	98.75	95.08	94.23	94.76	96.58
Cation Basis (O,OH,F)	23	23	23	23	11	11	11	11
Si	6.072	6.139	7.076	7.297	2.762	2.735	2.991	2.850
Ti	0.346	0.450	0.137	0.068	0.376	0.205	0.115	0.280
Al	2.048	2.073	0.660	0.475	1.229	1.407	1.000	1.108
Fe^{3+}	0.516	0.189	0.109	1.067	-	-	-	-
Fe^{2+}	0.604	1.192	0.427	0.381	0.699	0.479	0.798	0.874
Mn	0.022	0.026	0.181	0.261	0.002	0.000	0.037	0.021
Mg	3.393	2.932	3.411	3.451	1.706	2.077	1.999	1.743
Ca	1.840	1.861	1.576	1.507	-	-	-	-
Na	0.747	0.692	0.534	0.596	0.028	0.081	0.013	0.019
K	0.156	0.213	0.102	0.109	0.898	0.808	0.861	0.846

	Gabbro Plagioclase		Syenite Plagioclase	Syenite Perthite		Gabbro Pleonaste	Gabbro Magnetite	Gabbro Ilmenite
	CG-50[7]	CG-5[9]	CS-12[5]	CS-43[7]		CG-5[3]	CG-5[3]	CG-5[5]
SiO_2	51.4(12)	59.1(20)	65.1(6)	66.3(10)	TiO_2	0.13(31)	1.06(8)	51.9(11)
Al_2O_3	31.1(6)	25.2(9)	21.4(2)	19.8(2)	Al_2O_3	62.6(11)	0.65(5)	0.09(1)
FeO	0.20(3)	0.21(4)	0.29(27)	0.14(5)	Cr_2O_3	0.19(10)	0.28(2)	0.02(2)
CaO	12.8(8)	7.63(139)	2.77(12)	0.17(12)	$*Fe_2O_3$	4.68	58.6	4.82
Na_2O	4.02(55)	6.61(93)	9.63(39)	4.59(352)	FeO	18.8(7)	39.9(10)	37.5(2)
K_2O	0.13(2)	0.57(16)	0.27(26)	10.0(48)	MnO	0.21(5)	0.14(2)	3.13(10)
Total	99.67	99.29	99.46	100.48	MgO	14.6(5)	0.37(2)	2.91(10)
					Total	100.52	101.06	100.39
Cation Basis (O)	8	8	8	8	Cation Basis (O)	4	4	3
Si	2.341	2.657	2.877	2.996	Ti	0.003	0.031	0.960
Al	1.667	1.336	1.117	1.000	Al	1.922	0.028	0.002
Fe	0.006	0.008	0.010	0.005	Cr	0.004	0.008	-
Ca	0.622	0.367	0.131	0.008	Fe^3	0.092	1.709	0.089
Na	0.354	0.575	0.825	0.401	Fe^2	0.395	1.294	0.771
K	0.006	0.031	0.014	0.576	Mn	0.005	0.005	0.065
					Mg	0.569	0.021	0.107

All Fe is reported as FeO except for amphiboles, in which Fe_2O_3 was calculated by the method of Leake (1978), and for oxides, in which Fe_2O_3 was calculated from stochiometry.

Numbers in brackets [] are replicate analysis averaged.

Numbers in parentheses () indicate one standard deviation in terms of least units reported.

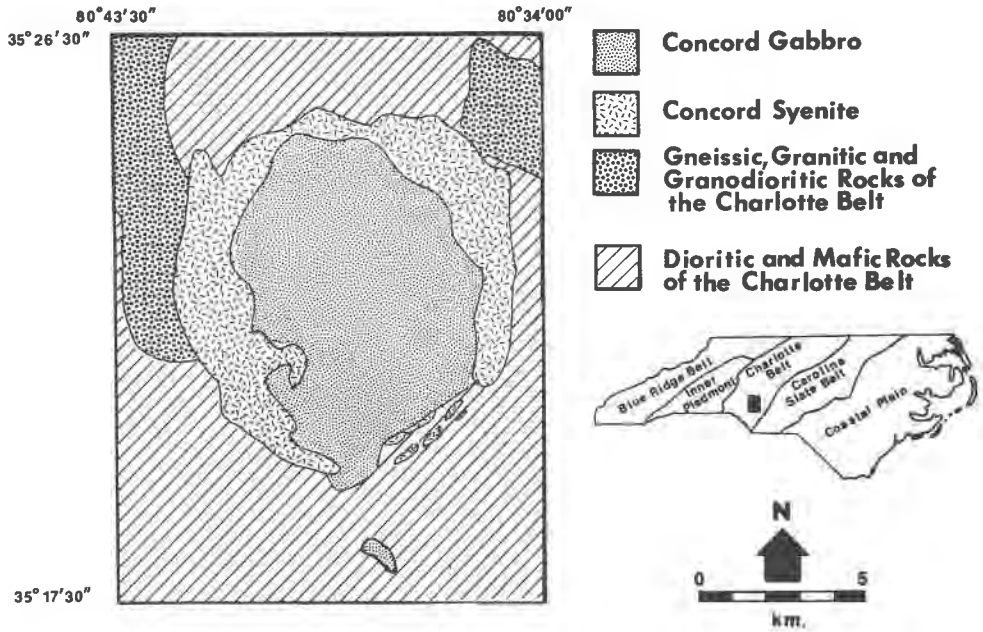

Fig. 1. Geologic map of the Concord intrusive complex, a compilation of this work and that of White and Mundorff (1944), LeGrand and Mundorff (1952), and Bell (1960). The inset map shows the location of the complex within the Charlotte belt in the North Carolina Piedmont.

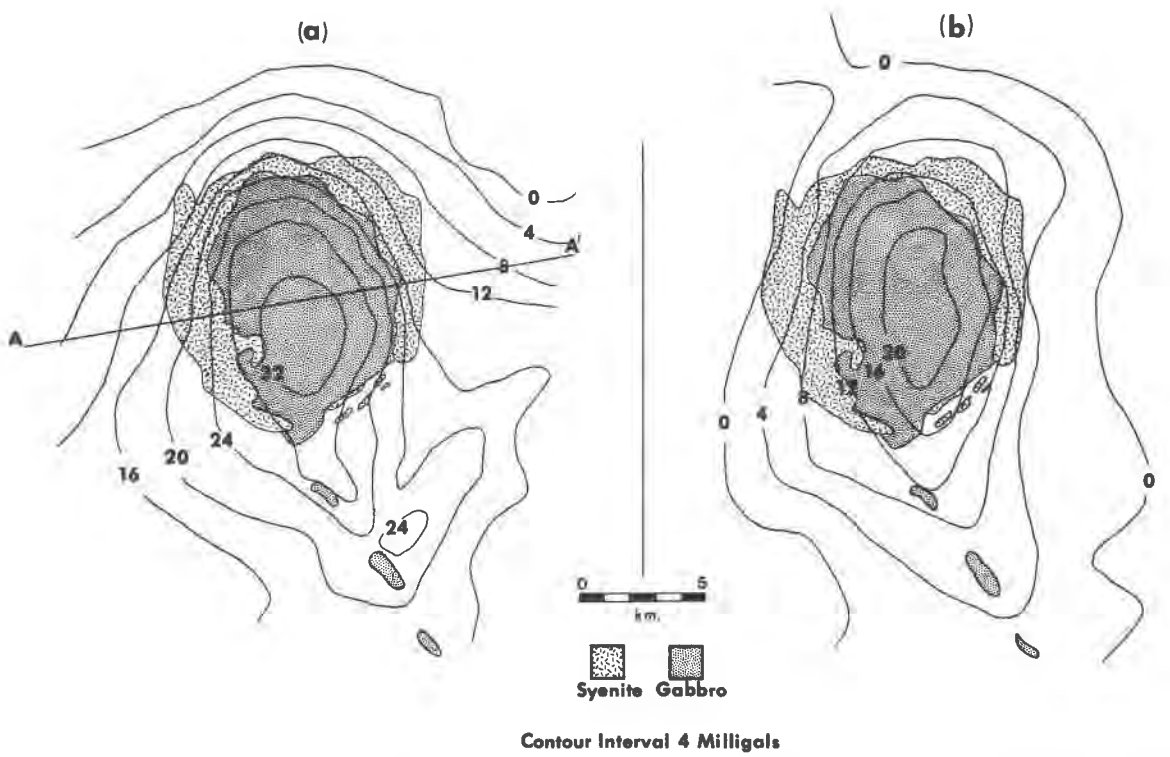

Fig. 2. Contoured gravity data (Morgan and Mann, 1964) superimposed on the surface outcrop pattern of the Concord gabbro–syenite complex. (a) Simple Bouger anomaly map. (b) Residual anomaly map. Line A–A′ in (a) was used to produce the gravity profile in Fig. 3.

used to estimate the shape of the body at depth. The residual anomaly map (Fig. 2b) represents the gravitational distribution of local, shallow geologic structures. The contours shown on this map roughly outline the shape of the pluton at the surface. The trend of isolated gabbro bodies extending from the open southern end of the complex is reflected in both gravity maps, suggesting these satellite intrusions are related to the main gabbro body at depth.

The detailed nature of this gravity study provides an opportunity to construct a gravity profile and propose a simple model of the geometry of the pluton at depth. An observed gravity profile was constructed along line A–A′, shown on the simple Bouguer anomaly map in Figure 2a. This particular line was chosen because it produced the most symmetrical profile (Fig. 3). Using the Talwani 2-D Gravity Program No. W9206 (Talwani *et al.*, 1959), several theoretical gravity profiles were constructed by varying the dip angle and direction of the syenite dike and the depth to the bottom of the pluton. Figure 3 illustrates the profile that most closely resembles the observed gravity profile along A–A′. The model which produced this profile depicts a steep-walled syenite ring dike with an outward dip of 78° on the west side and vertical dip on the east side, and a depth of about 6 km to the bottom of the complex. An even more refined fit might be obtained if the syenite were modeled as a wedge thickening downward rather than as a plate of uniform thickness.

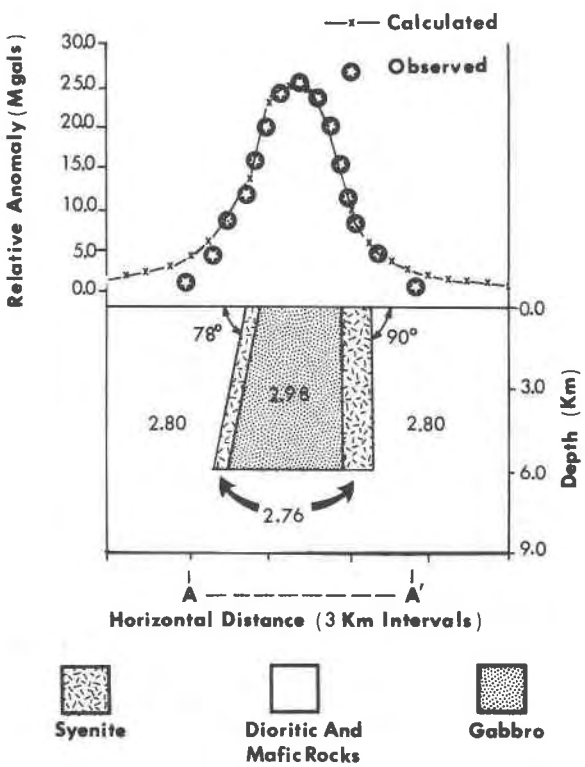

Fig. 3. Comparison between observed and calculated gravity profiles along section A–A′ in Figure 2a. The calculated profile assumes the geometry and rock densities indicated.

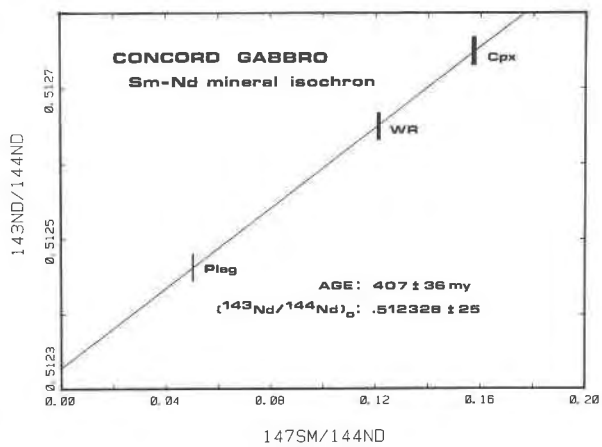

Fig. 4. Sm–Nd mineral isochron for Concord gabbro, defined by plagioclase and clinopyroxene separates and whole rock (WR).

Age dating and isotopic constraints

The three samples (clinopyroxene and plagioclase separates, whole rock) used to date the gabbro by the Sm–Nd technique give a near-perfect isochron age of 407±36 m.y. (1σ error, York, 1966), as shown in Figure 4. Sneeringer (1981) has measured diffusion rates of Sm in clinopyroxene which show that diffusive exchange of rare-earth elements involving this mineral (the major host of REE in the gabbro) is unlikely below magmatic temperatures. Closure temperatures above 850°C are indicated even for improbably slow cooling rates. We therefore interpret the mineral isochron age as the emplacement age of the gabbro. Rb–Sr whole-rock dating of the syenite, which also gives an emplacement age, was reported by Fullagar (1971) at 404±21 m.y. (recalculated using $\lambda^{Rb} = 1.42 \times 10^{-11}$/yr) and is identical within error to our result for the gabbro. Measurements are given in Table 3.

An important finding is that the Nd initial ratios as taken from the gabbro isochron (Fig. 4) and calculated for the syenite using the published Rb–Sr age are indistinguishable. The same is true for Sr initial ratios (Fullagar, 1971). These observations are consistent with a closed-system relationship between the gabbro and syenite and are strong evidence that the syenite was not derived by assimilation of any significant amount of crustal rock by magma similar in isotopic composition so that which formed the Concord gabbro. Such a process would result in elevation of initial $^{87}Sr/^{86}Sr$ of syenite relative to gabbro if typical older intermediate to upper crustal rocks were involved. Isotopic composition of potential lower crustal contaminating material may be inferred from Hercynian granitic rocks of the Charlotte belt, which probably derived a significant portion, if not all, of their mass from the lower crust. Published $^{87}Sr/^{86}Sr$ values for

Table 3. Results of isotopic analyses

Sample	$(^{143}Nd/^{144}Nd)_{measured}$	$(^{147}Sm/^{144}Nd)$	$(^{143}Nd/^{144}Nd)_{initial}$	$\varepsilon_{Nd}(t)$[1]
Concord gabbro CG-5			.512328 ± 25	+4.4 + 0.5
plagioclase	.512463 ± 17	.0504		
whole rock	.512650 ± 18	.1212		
clinopyroxene	.512749 ± 17	.1574		
Concord syenite CS-0	.512595 ± 20	.1049	.512318 ± 37[2]	+4.2 ± 0.9[2]

1. $\varepsilon_{Nd}(t) = [\frac{(^{143}Nd/^{144}Nd)_{sample,\ t}}{(^{143}Nd/^{144}Nd)_{CHUR,\ t}} - 1] \times 10^4$ Parameters used for calculating CHUR evolution: $^{147}Sm/^{144}Nd = .1967$ $(^{143}Nd/^{144}Nd)_{today} = .512622$

2. Error incorporates 1-σ error in Rb/Sr age. All other errors are 2-σ.

these plutons (Fullagar, 1971; Jones and Walker, 1973; Fullagar and Butler, 1979) indicate that Sr isotopes would be a poor indicator of crustal contamination at depth, since several of them have low initial ratios, some very close to the value for the Concord gabbro/syenite. Investigation of Nd isotopic composition of the granitic plutons has shown them to have strong "crustal" signatures, with average initial $\varepsilon_{Nd} = 2.5$ (Sando and Hart, 1982). This requires a lower crust at least as depleted as these values with respect to $^{143}Nd/^{144}Nd$ and is consistent with calculations of lower crustal isotopic composition based on probable age of the crust and reasonable guesses about its Sm/Nd. These values are quite different from those measured in the Concord rocks; assimilation of lower crustal material would thus lower the $^{143}Nd/^{144}Nd$ of an assimilating magma with isotopic composition like that of the gabbro. Nd concentrations measured in the gabbro (40 ppm) are probably lower than those of the potential crustal contaminant. Even for the case where they are equal, calculations using the granitoid isotopic composition for the contaminant result in a upper limit of 20% assimilated material when errors in our initial ratio determinations are taken into account. The limit is conservative, since the isotopic contrast between crust and gabbro may be greater, and because of the assumptions of equal concentrations. The combined use of the Nd and Sr isotope systems therefore permits both upper and lower crustal contamination of the Concord parental magma to any large extent to be ruled out.

A model for emplacement of the complex

The identical crystallization ages for the Concord gabbro and syenite indicate that these units were associated in time as well as space. A reasonable sequence of events that would produce the structure of the Concord complex begins with the intrusion of mafic magma to form a gabbro stock. This pulse of magma would be derived from a large reservoir of magma at depth prior to significant fractionation. The syenitic magma was not produced at the present erosional level, because no intermediate rocks occur, but could have formed by fractionation of the source magma body at depth. A fractured region around the contact between the gabbro and country rock was subsequently intruded by this syenitic magma. As noted by Morgan and Mann (1964), the syenite ring dike probably did not form as a result of subsidence of a central gabbroic block into syenitic magma, because the magnitude of the residual gravity anomaly is inconsistent with this geometry and because subsidence of many kilometers of the steep-walled gabbro stock would be required to provide room for a ring dike of the observed width. The incompleteness of the ring dike may be related to the presence of small, satellite gabbro bodies extending from the open southern end of the pluton. The geophysical maps suggest that these bodies may be continuous at depth with the Concord gabbro body, possibly representing outcrops of a dike-like projection of gabbro. Subsolvus crystallization of alkali feldspars in the syenite indicates the complex was emplaced at depths of approximately 15 km or greater. We will now examine the petrographic and geochemical characteristics of gabbro and syenite in order to devise and test a fractionation model relating the two lithologies, as proposed above.

Petrology of the gabbro

Concord gabbro samples are medium-grained meso- and orthocumulates consisting primarily of plagioclase, olivine, clinopyroxene, orthopyroxene, and amphibole, with lesser amounts of biotite, oxide and sulfide minerals, apatite, and alteration products. Three major gabbroic rock types are distinguished by the presence of different cumulus minerals. (*Cumulus* is used here only as a textural term to describe discrete crystals and does not necessarily imply settled crystals (Irvine, 1982)). The first type contains cumulus olivine and plagioclase poikilitically enclosed by postcumulus orthopyroxene, clinopyrox-

ene, and hornblende (Fig. 5a); this type is referred to as olivine–plagioclase cumulate (OPC) gabbro. The second gabbroic rock type is a clinopyroxene–plagioclase cumulate (CPC) in which these phases are poikilitically enclosed by postcumulus orthopyroxene and hornblende (Fig. 5b). In this rock type clinopyroxene does not occur as oikocrysts. Samples which contain all three cumulus phases are olivine–clinopyroxene–plagioclase cumulates (OCPC) and are rather uncommon. Areal distributions of OPC, CPC, and OCPC samples within the pluton appear to be non-systematic (Olsen, 1982).

Modal proportions of the major phases (Table 1) can be compared using the classification diagrams devised by Streckeisen (1973). The gabbroic rocks are norites and gabbronorites, according to modal clinopyroxene/orthopyroxene ratios (Fig. 6). CPC and OCPC samples generally plot within the gabbronorite field of Figure 6, whereas OPC samples plot as norites and gabbronorites. For simplicity only the term *gabbro* with appropriate modifiers to indicate cumulus phases will be used here for classification, because the identification of cumulus phases is central to reconstructing fractionation patterns.

Plagioclase is the dominant mineral in gabbro samples. Individual grains are normally zoned and partially altered

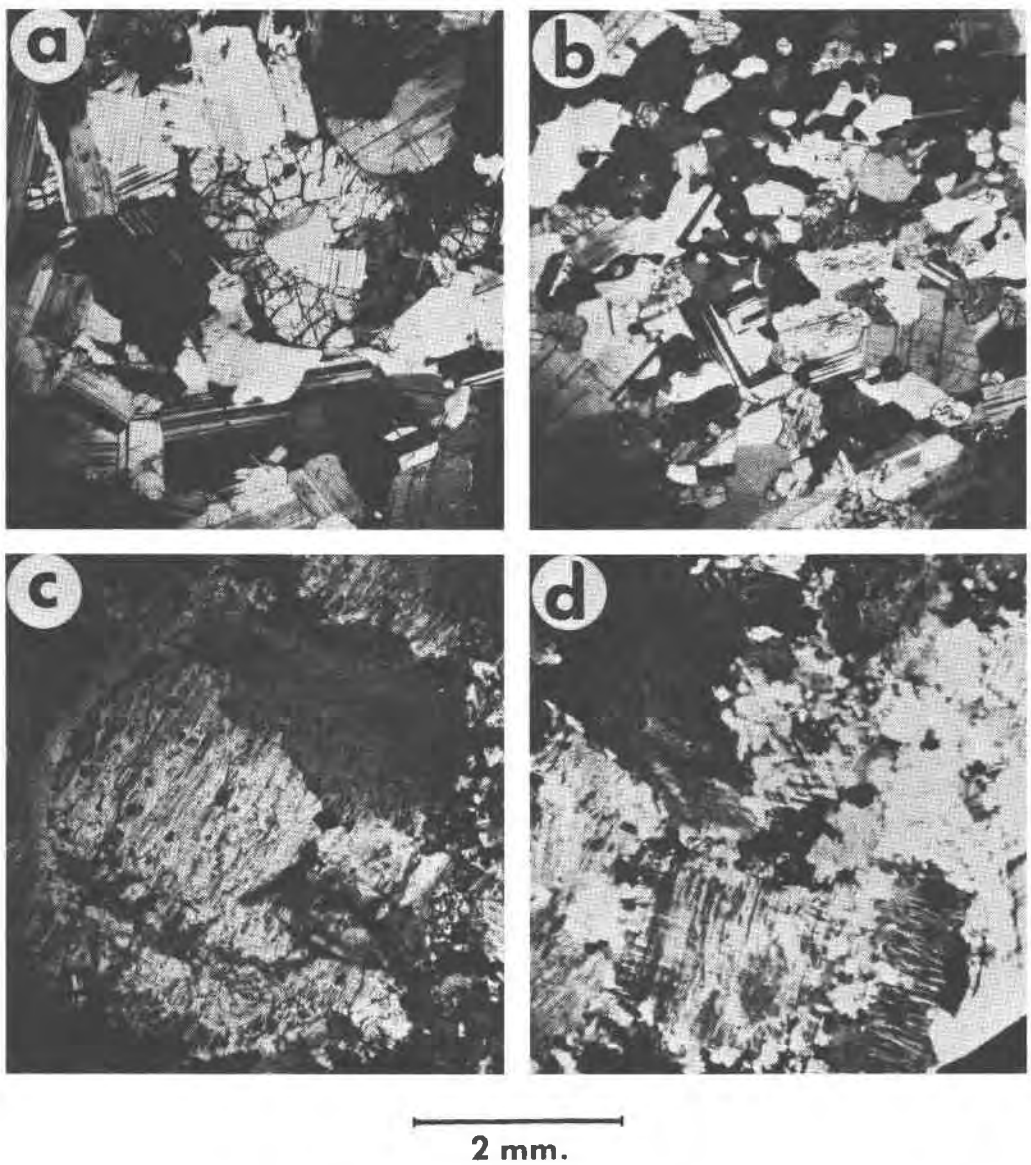

Fig. 5. Photomicrographs of samples from the Concord complex in cross-polarized, transmitted light. (a) Cumulus olivine and plagioclase in OPC gabbro. (b) Cumulus clinopyroxene and plagioclase and postcumulus amphibole in CPC gabbro. (c) Zoned perthite phenocryst with augite and Fe–Ti oxide inclusions in syenite. (d) Porphyritic texture in syenite, with perthite phenocrysts and groundmass of plagioclase, microcline, quartz, and interstitial augite, amphibole and oxides.

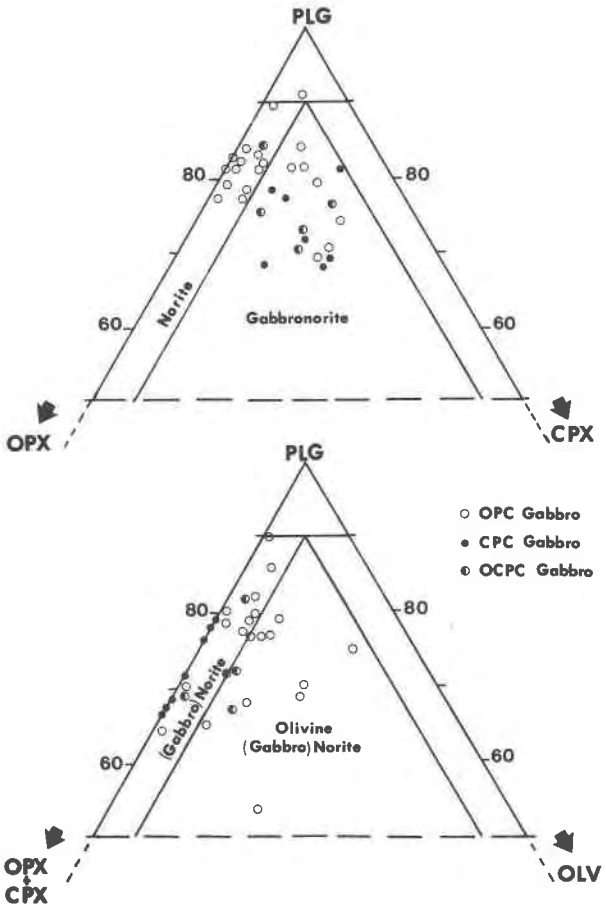

Fig. 6. Modal variations in gabbroic rocks. Nomenclature is that of Streickesen (1973).

to sericite. Plagioclase in the gabbro pluton ranges in composition from An_{77-31}, but the range is much more restricted within any specific sample (Fig. 7). The most calcic plagioclase occurs in OPC gabbros, and the least calcic in CPC gabbros.

Olivine within the gabbro ranges in composition from Fo_{78-70} (Fig. 8), but grains have uniform composition within any one specimen. Olivine in OPC gabbros is more magnesian than that in OCPC gabbros. Most grains are subhedral to anhedral and are replaced along fractures by magnetite and serpentine. Some grains are rimmed by orthopyroxene and hornblende.

Clinopyroxene occurs as oikocrysts surrounding plagioclase and olivine in OPC gabbro, and as discrete subhedral to anhedral grains in CPC and OCPC gabbros. This mineral is diopsidic augite (Fig. 8), and grains within the same section all have the same composition. Clinopyroxene contains exsolution lamellae of orthopyroxene parallel to (100), as well as thin platelets of magnetite and ilmenite parallel to (010).

Orthopyroxene occurs as large oikocrysts in all gabbroic rock types. These bronzites (Fig. 8) are homogeneous in composition but contain exsolution lamellae of clinopyroxene along (100). Orthopyroxene also forms thin reaction rims around some olivines and symplectic intergrowths with magnetite and ilmenite. This symplectite normally occurs at the edges of olivine grains that are surrounded by hornblende, an indication that the intergrowth is a result of reaction between olivine and residual melt (Ambler and Ashley, 1980; McSween, 1980). Platelike lamellae of ilmenite oriented along (010) also occur in the orthopyroxene. In OPC and OCPC gabbros, orthopyroxene is more magnesian than in CPC gabbros.

Large oikocrysts of hornblende are strongly pleochroic from reddish-brown to tan. Compositions of amphiboles in terms of Ca, Mg and Fe are shown in Figure 8. According to the classification system of Leake (1978), the gabbroic amphiboles are pargasites and magnesiohastingsites. These amphiboles appear to have formed primarily by late-magmatic replacement of postcumulus pyroxenes.

Biotite occurs as tabular sheaths or as rims around oxide minerals. Gabbroic biotites appear to show sympathetic enrichments of Ti and Fe (Fig. 8).

Magnetite and ilmenite occur as interstitial subhedral grains or as euhedral to subhedral inclusions in cumulus and postcumulus minerals. Thus some oxide grains may be cumulus phases. Composite magnetite and ilmenite grains are commonly joined by a boundary, along which a thin discontinuous rim of pleonaste is found. Some magnetite grains contain thin straight lamellae of ilmenite. Compositions of typical grains are shown in Table 3.

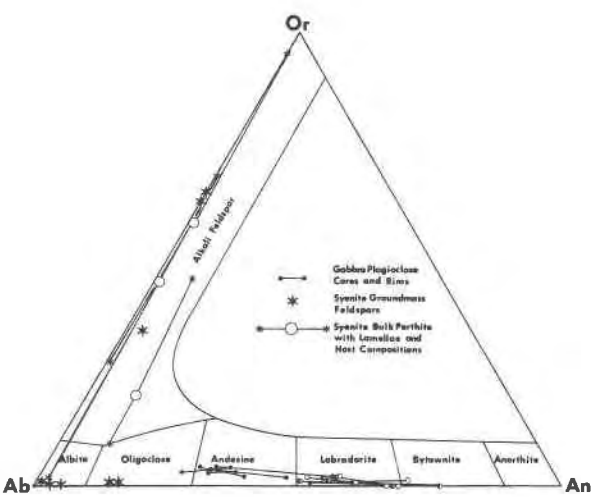

Fig. 7. Molar compositions of feldspars in Concord gabbro and syenite. Individual zoned plagioclase core and rim compositions in gabbro samples are joined by tie–lines along the Ab–An join. A key for symbols for different gabbro types is given in Fig. 6. Bulk perthite compositions in syenite (large open circles) are joined to corresponding lamellae and host compositions by tie lines along the Ab–Or join. Groundmass feldspars in syenite plot near Ab or along the Ab–Or join.

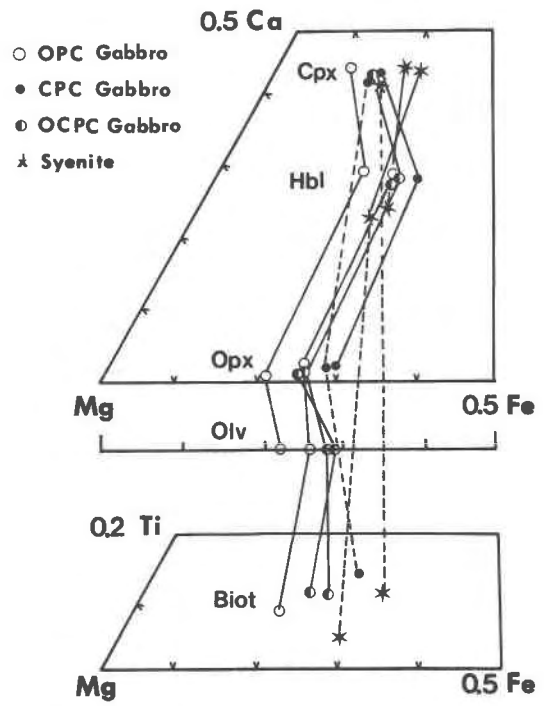

Fig. 8. Molar compositions of ferromagnesian silicates in the Concord gabbro and syenite. Minerals (clinopyroxene, hornblende, orthopyroxene, olivine, biotite) coexisting in the same samples are joined by tie-lines. All of these phases are homogeneous.

Sulfide minerals occur as round blebs in gabbroic samples. Pyrrhotite, the dominant sulfide phase, is associated with lesser amounts of pyrite, chalcopyrite and pentlandite.

Other accessory minerals include apatite, which forms euhedral laths and prisms, mostly interstitial, but also as inclusions in feldspars. Minute zircon inclusions in biotite produce pleochroic haloes. Plagioclase grains contain veinlets and patches of sericite as an alteration product, and chlorite and serpentine are present as alteration products of pyroxene and olivine.

Petrology of the syenite

The Concord syenite is a coarse-grained, seriate porphyry containing large phenocrysts of perthite and antiperthite (Fig. 5c) in a groundmass of perthite, plagioclase, microcline, clinopyroxene, biotite, amphibole, quartz, oxide and sulfide minerals, zircon, apatite and monazite (Fig. 5d). Modal proportions of the major minerals (Table 1) fall within the syenite field of the I.U.G.S.-approved classification diagram (Streckeisen, 1973).

Feldspar megacrysts range up to 2 mm in length and commonly stand out in relief on weathered surfaces of syenite. Perthite and antiperthite can be distinguished in stained syenite thin sections and slabs, but in unstained samples it is difficult to determine which component is the host mineral and which is the exsolved phase. Some perthitic feldspars are strongly zoned, with perthitic cores surrounded by bands of sodic plagioclase, followed again by perthitic rims. Many megacrysts contain dusty zones of sericite and clay inclusions. Clinopyroxene, apatite and oxide minerals are present as inclusions. The bulk compositions of perthite and antiperthite megacrysts (determined by averaging a number of defocussed beam analyses) are joined to their corresponding lamellae and host compositions by tie lines in Figure 7. The compositions of alkali feldspar and sodic plagioclase are similar in perthites and antiperthites.

Feldspars in the groundmass are plagioclase (An_{1-16}) and microcline. The compositions of these phases (Fig. 7) are similar to those in perthitic megacrysts. Quartz occurs within the groundmass, mostly as myrmekitic intergrowths with albite. However, one analyzed sample (CS-88, Table 1) contains sufficient anhedral quartz grains to be classified as granitic.

Mafic and opaque minerals in the syenite tend to occur as intergranular clusters between megacrysts. Clinopyroxene grains are anhedral, fractured, and commonly rimmed by brown amphibole. A green amphibole occurs as discrete anhedral to subhedral grains. Syenite clinopyroxenes are more Fe-rich than those in gabbros, and syenite amphiboles have lower Ca contents than the corresponding phases in gabbros (Fig. 8). These amphiboles are magnesio- and actinolitic hornblendes in the terminology of Leake (1978). Biotite is present in small amounts as ragged flakes clustered with other mafic minerals. Biotite in the syenite is pleochroic in shades of reddish-brown to brown or pale green to green; only the reddish-brown variety occurs in gabbro. Biotite in syenites is more Fe-rich and Ti-poor than in gabbro (Fig. 8). Anhedral magnetite, ilmenite and pyrite grains are also associated with mafic clots, along with accessory apatite, zircon, and monazite.

Crystallization history of the complex

In OPC gabbro, cumulus olivine and plagioclase are enclosed by postcumulus orthopyroxene, clinopyroxene and hornblende. Clinopyroxene joined the other crystallizing cumulus phases in OCPC gabbro. With further fractionation olivine ceased to crystallize because of a reaction relationship with the melt to form orthopyroxene. In CPC gabbro, clinopyroxene and plagioclase are cumulus minerals, surrounded by postcumulus orthopyroxene and hornblende. This textural sequence implies formation of cumulate rocks in the following order: OPC, OCPC, CPC. This sequence is corroborated by Fe-enrichment trends in ferromagnesian minerals and Na-enrichment trends in plagioclase cores (Figs. 7,8).

This evidence indicates that olivine and plagioclase were the first minerals to crystallize from the parental magma. Inclusions of Fe-Ti oxides within cumulus phases imply that these may have also crystallized early. The

crystallization sequence was joined later by clinopyroxene. Postcumulus material crystallized to form oikocrysts of clinopyroxene and orthopyroxene in early cumulate rocks, or orthopyroxene only in later cumulates. Hornblende probably formed by late magmatic replacement of postcumulus pyroxene. Biotite also crystallized from the magma late in the sequence, or by reaction of oxides with residual melt.

If the Concord gabbro formed from magma tapped from a larger reservoir at depth before significant fractionation had occurred, the gabbroic crystallization sequence reflects the subsequent crystallization sequence in the larger chamber as well. The fractionation of this parental magma thus may have been controlled by crystallization of plagioclase, olivine, and clinopyroxene, possibly with minor oxide phases. Because most samples (OPC and CPC gabbros) contain only two of the three major cumulus phases it is difficult to estimate the relative proportions of these three minerals in the fractionating assemblage. The average modes for each rock type and for all gabbro samples are presented in Table 4; however, it is uncertain whether an average mode for all samples weighs the various types of cumulates in their proper volumetric proportions. Olivine and clinopyroxene occur approximately in a cotectic ratio (Table 4), but plagioclase is overabundant. It is clear that some of the plagioclase is postcumulus, formed as zoned overgrowths on cumulus crystals or as crystals nucleated from intercumulus liquid. The proportions of the fractionating phases may be better estimated from the geochemical arguments that follow.

Fractionation of major elements

The following necessary assumptions underlie conclusions drawn from this and the following sections: (1) The Concord syenite was not derived by fractionation from the Concord gabbro *in situ*, but both may have been derived from a common parental magma at depth. It is assumed that the magma that formed the gabbro was extracted from such a chamber before significant fractionation occurred. Thus the identity and compositions of the cumulus minerals in the Concord gabbro would be the same as those in the larger fractionating parental magma chamber, in the absence of significant pressure effects. (2) It is assumed that the averages of all analyzed samples of gabbro and of syenite represent the bulk compositions of these two magmas. Because the gabbro samples are cumulate rocks, this approximation is not rigorously correct, especially for trace elements.

In any chemical fractionation diagram relating Concord gabbro and syenite, there is a gap between clusters of points because there are no samples with intermediate compositions. For this reason the exact differentiation path between gabbro and syenite cannot be determined. However, the identification of crystallizing phases that may have dominated the fractionation sequence can be estimated from major element chemistry and mineralogy of the two end-members. Four representative two-element variation diagrams are illustrated in Figure 9 (a–d), using average gabbro and syenite compositions (Table 5). These variations have been interpreted using the extraction method of Cox *et al.* (1979). Average mineral compositions for olivine and clinopyroxene and the average plagioclase composition from the samples with the most calcic plagioclase (Table 5) were used to construct the extract polygons (triangles in Figure 9, a–d). The average syenite composition can be produced by fractionation of plagioclase + olivine + clinopyroxene, as the extract composition in each of these diagrams falls within the polygon they define, but syenite cannot be produced by

Table 4. Relative proportions of cumulus minerals

	OPC Modes (20)	CPC Modes (7)	OCPC Modes (6)	Avg. Modes[1]	Cotectic Proportions[2]	Extract Diagrams[3]	Mixing Program[4]
Plag	86	81	84	84	55-60	57-61	57
Olv	7	-	11	5	10-15	13-25	19
Cpx	*6	18	5	10	25-30	15-30	18
Mt	0.5	0.9	0.1	0.7	-	-	4
Ilm	0.5	0.3	0.1	0.3	-	-	2

Units in () represent number of samples point-counted. Values are recalculated to 100%.

1. Average modes are weighted averages of all gabbro point counts.
2. Cotectic proportions from McCallum et al. (1980).
3. Ranges of mineral proportions estimated from Figure 11e.
4. Computed mineral proportions from the petrologic mixing calculation (Table 6).

*All Cpx in OPC gabbro is post-cumulus.

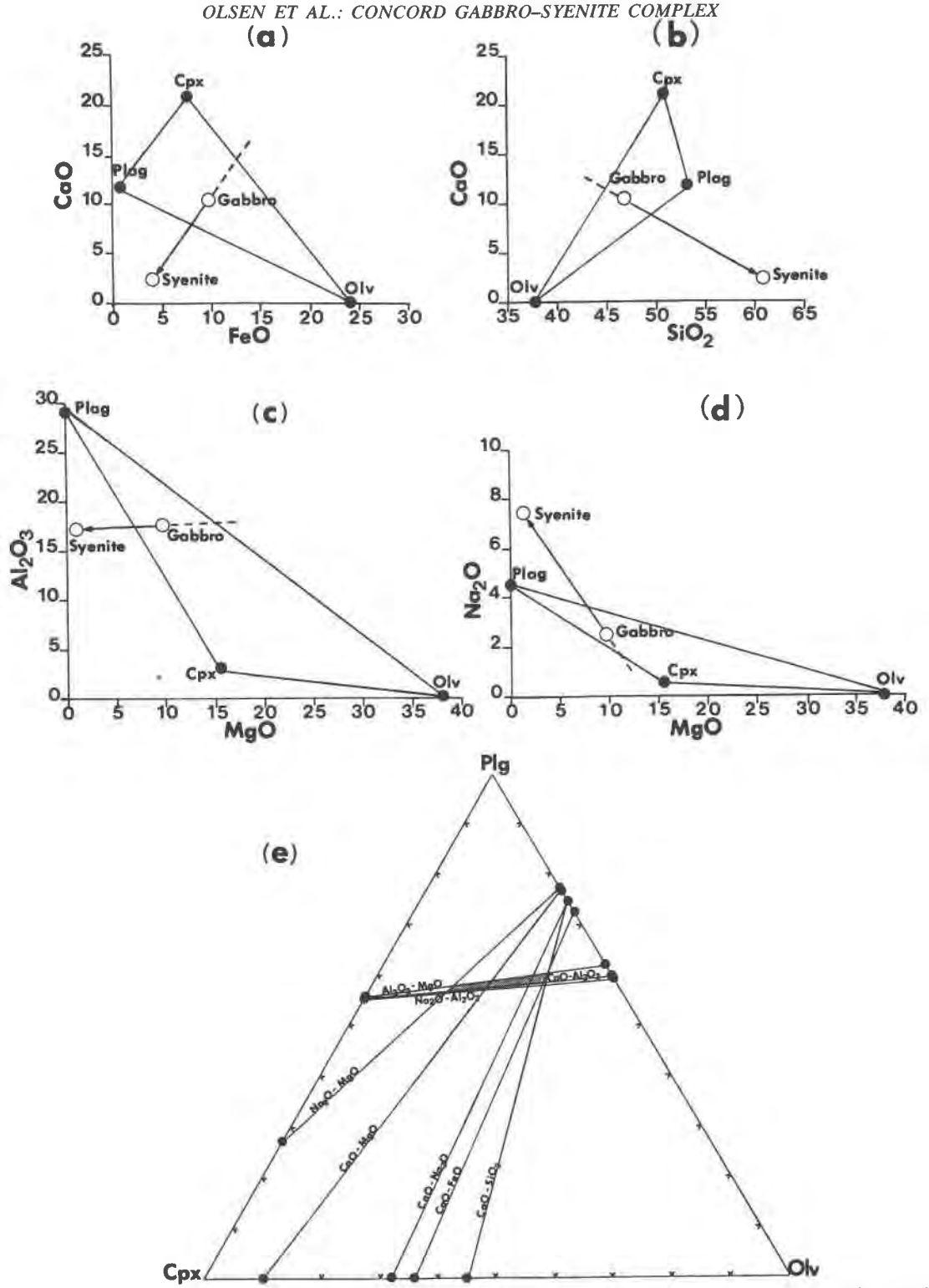

Fig. 9. (a–d) Four representative two-element variation diagrams showing the inferred gabbro–syenite fractionation trends (solid arrows). In each diagram this trend can be produced by extracting (dashed lines) mixtures of plagioclase, clinopyroxene, and olivine with the same compositions as observed cumulate gabbro phases. Compositions of average gabbro, syenite, plagioclase, clinopyroxene, and olivine used in constructing these diagrams are given in Table 5. (e) Estimation of the relative proportions of plagioclase, clinopyroxene and olivine required to produce the gabbro–syenite trend in eight extraction diagrams. The region in which the lines intersect (shaded area) represents the range of mineral proportions in the assemblage most likely to have produced this fractionation pattern.

Table 5. Average compositions (weight % oxides) of Concord gabbro and syenite and presumed cumulus phases used in geochemical computations

	MnO	FeO[1]	K_2O	CaO	TiO_2	Na_2O	MgO	Al_2O_3	SiO_2	Total
Syenite	0.19(0.02)	3.95(1.05)	4.41(1.23)	2.26(1.21)	1.05(0.29)	7.45(0.49)	1.27(0.64)	17.10(0.40)	60.8(2.20)	98.48
Gabbro	0.14(0.03)	9.73(1.88)	0.31(0.19)	10.47(1.02)	1.20(0.38)	2.51(0.29)	9.59(2.00)	17.59(1.80)	46.9(1.50)	98.44
Olivine	0.49	23.95	-	-	-	-	38.07	-	37.54	100.05
Plagioclase[2]	-	0.24	0.23	11.76	-	4.43	-	29.45	53.19	99.30
Plag (An 70)[3]	-	0.23	0.08	14.04	-	3.29	-	31.39	50.01	99.04
Plag (An 39)[3]	-	0.21	0.57	7.63	-	6.61	-	25.20	59.07	99.29
Clinopyroxene	0.46	7.43	-	21.23	0.85	0.55	15.39	3.19	50.95	100.05
Magnetite	-	90.51	-	-	3.54	-	0.50	0.77	-	95.32
Ilmenite	-	41.66	-	-	51.92	-	2.91	0.09	-	96.58

Average syenite and gabbro values from data of Cabaup (1969) and Butler and Ragland (1969). Units in () represent one standard deviation.

Average mineral compositions from electron microprobe analyses (Olsen, 1982).

1. Total Fe as FeO.

2. Average of plagioclase analyses from sample with most calcic plagioclase (used in Figure 11).

3. Most sodic and calcic plagioclases measured (used in the petrologic mixing program, Table 6).

fractionation of any two of these phases. This conclusion is in agreement with previous textural evidence that suggested all three minerals are cumulus phases in the gabbro. The extraction diagrams are also consistent with fractionation of a four-phase assemblage plagioclase + olivine + clinopyroxene + orthopyroxene, but this fractionation is not considered plausible because orthopyroxene in the Concord gabbro is postcumulus and probably was never of major importance in the crystallizing assemblage.

Each extraction diagram gives a range of proportions for each mineral in the crystallizing assemblage. Figure 9e illustrates the proportional ranges given by 8 such variation diagrams. This figure was constructed by determining the range of extract compositions given by each extraction diagram, and plotting each range on an equilateral plagioclase–olivine–clinopyroxene triangle. The region in which lines intersect (shaded) is taken to be the range of mineral proportions in the assemblage most likely to produce the gabbro–syenite fractionation.

The validity of this fractionation model was put to a more quantitative test using the least squares petrologic mixing calculations described by Wright and Doherty (1970). Average compositions of gabbro and syenite and the same compositions of clinopyroxene and olivine used above (Table 5) were employed in the calculations. The plagioclase composition was allowed to "float" between the most calcic (An 70) and the most sodic (An 39) observed values in the gabbro (Table 5). Addition of Fe-Ti oxides to the calculation resulted in an improved fit; textural evidence has already been cited that these may have been cumulus phases as well. The computed solution (Table 6) calls for removal of 95% by weight of a cumulate assemblage consisting of 57% plagioclase (average An 62), 19% olivine, 18% clinopyroxene, 4% magnetite and 2% ilmenite from the average gabbro composition to produce a residual melt of the average syenite composition. The sum of the squares of the residuals (0.053) is low, and the error values are reasonable. The largest error is in the Na_2O value (Table 6). To balance Na_2O, the fractionating plagioclase should be more calcic. This small imbalance is produced by the inability to balance SiO_2, possibly because of an analytical error in SiO_2 or Na_2O. The proportions of cumulus phases given by this method compare well with the values determined from major element extraction diagrams and, considering the uncertainties in these calculations, differ little from cotectic proportions (Table 4).

Fractionation of trace elements

Figure 10 presents average trace element contents and standard deviations for 6 gabbro and 7 syenite samples (Price, 1969) versus Differentiation Index, D.I. (normative Q + Or + Ab + Ne + Lc). It is difficult to specify how fractionation affected these trace element contents because the concentrations in the original liquid are not precisely known. The average Concord gabbro trace element contents are taken to approximate those of the parent magma. We attempt here only to determine if trace element patterns are qualitatively consistent with the fractionation model discussed above.

In Figure 10, Zr and the alkalis K, Rb and Li are enriched in the syenite relative to the gabbro, whereas all other analyzed trace elements are depleted. Fractionation of a spinel phase and a sulfide phase are suggested by depletion of Cr and V, and of Cu and Zn, respectively.

Table 6. Solution to the petrologic mixing problem

	Syenite	Olivine	Clinopyroxene	Magnetite	Ilmenite	Plagioclase	Observed Gabbro	Calculated Gabbro	Residuals
SiO_2	61.86	37.71	51.16	0.00	0.00	52.78	47.72	47.62	0.10
Al_2O_3	17.40	0.00	3.21	0.81	0.10	30.10	17.90	17.86	0.04
FeO[1]	4.02	24.06	7.47	94.96	43.14	0.23	9.90	9.86	0.05
MgO	1.30	38.24	15.46	0.53	3.02	0.00	9.76	9.76	0.01
CaO	2.30	0.00	21.32	0.00	0.00	12.54	10.66	10.67	-0.01
Na_2O	7.58	0.00	0.56	0.00	0.00	4.17	2.56	2.75	-0.19
K_2O	4.49	0.00	0.00	0.00	0.00	0.21	0.32	0.34	-0.02
TiO_2	1.07	0.00	0.86	3.72	53.76	0.00	1.23	1.18	0.05
Total	100.02	100.01	100.04	100.02	100.02	100.03	100.05	100.04	Σr^2= 0.0533
Solution	5.01	18.11	17.46	3.36	1.59	54.50 (An 62)			
Error[2]	1.1	0.3	0.7	0.1	0.2	0.7			
Composition of Cumulate Fraction[3]		19	18	4	2	57			

1. Total Fe as FeO.

2. Error estimated by empirical procedure of Wright and Doherty (1975).

3. Composition recalculated to 100%.

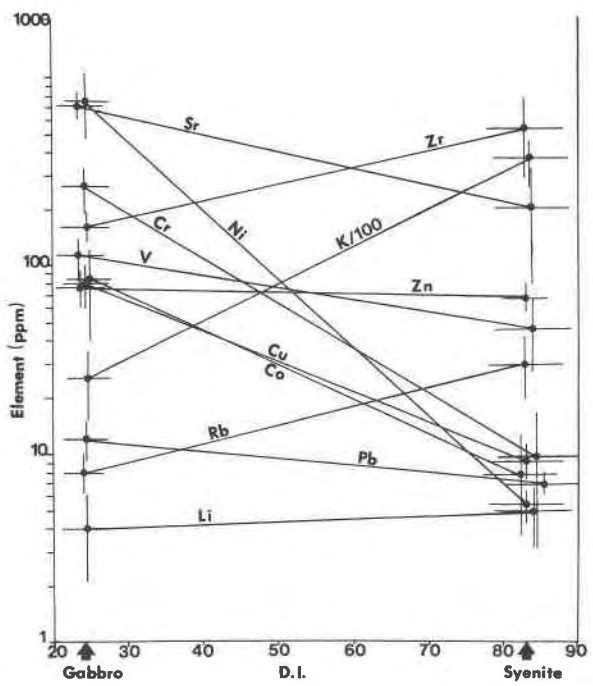

Fig. 10. Trace element variations between average Concord gabbro and syenite versus Differentiation Index (D.I.) Data obtained by Price (1969) were averaged and tabulated by Olsen (1982). Vertical and horizontal bars represent one standard deviation.

That a spinel phase was part of the fractionating assemblage is suggested from textural observations and petrologic mixing calculations. The bleb-shaped clusters of sulfide phases in gabbros suggest that an immiscible sulfide phase may have separated from the liquid at an early stage as well.

Two simple models describing the behavior of trace elements during fractional crystallization, Rayleigh (or perfect) fractional crystallization and equilibrium crystallization, have been used to constrain the degree of fractional crystallization and the identity and proportions of crystallizing phases required to produce a particular residual melt. The Rayleigh fractional crystallization equation produces a straight line on a logarithmic plot comparing two trace element concentrations, and the equilibrium crystallization equation produces a curved line.

In Figure 11(a,b), logarithmic plots of Rb versus Sr and Rb versus Zr in Concord gabbro and syenite are presented. In both cases the gabbro–syenite trend coincides with the calculated vector along which a melt fractionating plagioclase, olivine, clinopyroxene, and magnetite by Rayleigh fractional crystallization occurs. The least squares fractionation calculation indicated that 95% fractionation by weight of the given cumulus assemblage was required to produce a melt of average syenitic composition from the average gabbro composition. The vector lengths for Rayleigh fractionation in Figure 11 (a,b) are in

qualitative agreement, indicating degrees of fractionation of 85% and 80%, respectively. An even better agreement with calculations for major elements may be obtained if fractionation is modeled as some combination of Rayleigh and equilibrium processes (the latter produces shorter vectors at 95% fractionation). Although a small amount of biotite fractionation is permitted from trace element data, it seems unlikely because all biotite in the gabbro is postcumulus and syenite contans very little biotite. Thus trace element concentrations in gabbro and syenite are qualitatively consistent with the proposed fractionation model derived from petrography and major element chemistry.

Parental magma and fractionation path

In order to understand the fractionation scheme that relates the Concord gabbro and syenite, it is important to estimate the composition of the parental magma. The

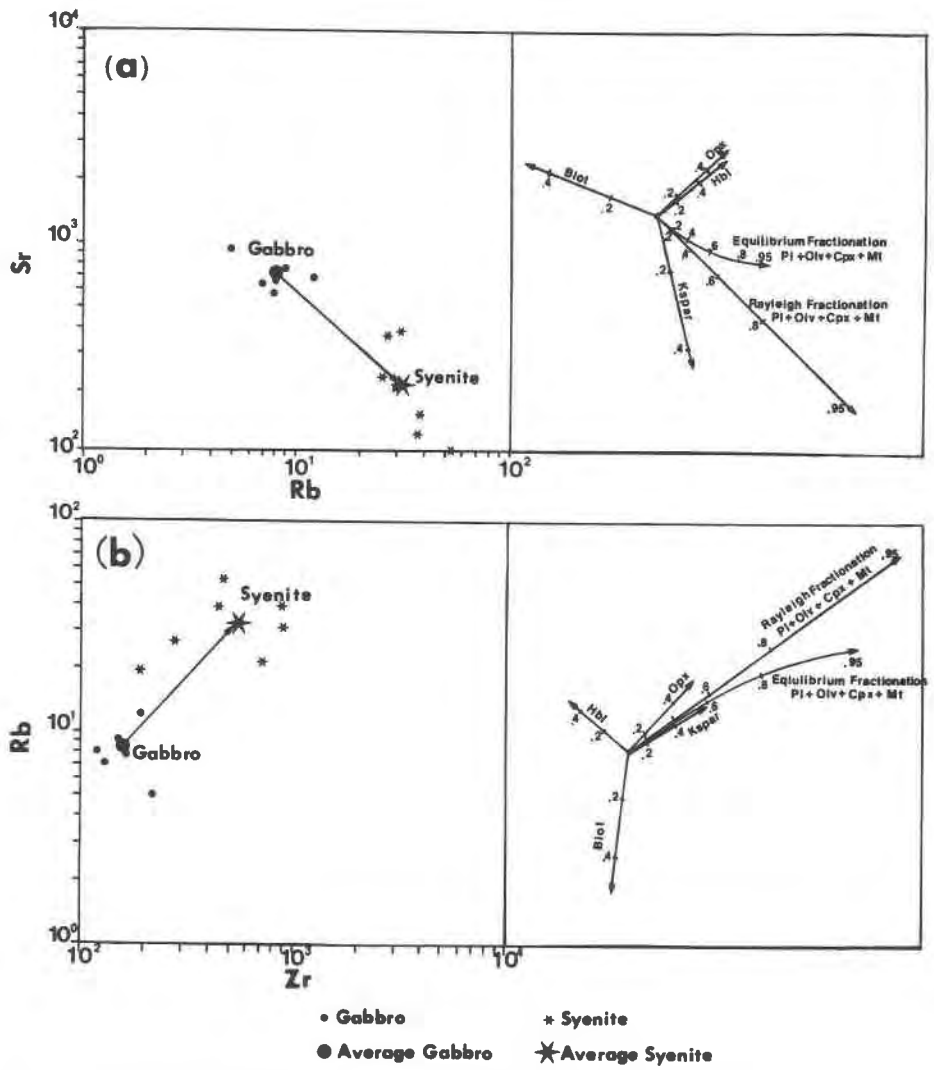

Fig. 11. (a) Rb–Sr and (b) Rb–Zr variation diagrams (ppm) for individual samples and average values of Concord gabbro and syenite. The vector diagrams to the right show the effects of crystallizing the assemblage plagioclase + olivine + clinopyroxene + magnetite in the proportions indicated by the petrologic mixing program (Table 6), as well as the effects of other possible fractionating phases. Both Rayleigh and equilibrium fractionation trends, calculated using the equations of Gast (1968) and Greenland (1970), are illustrated for the proposed fractionating assemblage. Distribution coefficients for Rb, Sr, and Zr for various phases depend on liquid composition; for these vector calculations an average value for silica (55%) intermediate between that for average gabbro (48%) and syenite (61%) was chosen. These values (Arth, 1976; Cox *et al.*, 1979; Pearce and Norry, 1979) are as follows:

	amph	*biot*	*mt*	*plag*	*cpx*	*olv*	*opx*	*kspar*
K_D^{Rb}	0.15	3.26	0	0.48	0.001	0.001	0.022	0.34
K_D^{Sr}	0.25	0.12	0	2.84	0.29	0.001	0.017	3.87
K_D^{Zr}	1.00	1.20	0.20	0.015	0.14	0	0.05	0

Concord gabbro samples almost certainly represent cumulate rocks (albeit containing significant postcumulus material), so it is unlikely that whole rock analyses precisely represent liquid compositions. This can be seen in Figure 12, in which calculated norms of 45 analyzed gabbro samples (data from Cabaup, 1969 and Butler and Ragland, 1969) do not fall within the circled fields of either alkaline or tholeiitic basalts. Fractionation of olivine + plagioclase + clinopyroxene will displace these samples relative to the Ol–Di join in this figure, along which many of them presently cluster. Therefore, it seems likely that the parental liquid must have been tholeiitic, although picritic or transitional basalt compositions cannot be ruled out.

Morse (1980), in a discussion of what he termed the "syenite problem", questioned the ability of a basaltic liquid with composition even slightly deviant from the critical plane of silica undersaturation (Fo–Di–Ab) in the normative basalt tetrahedron to produce a trachytic (syenitic) liquid. In the system $NaAlSiO_4$–$KAlSiO_4$–SiO_2 at low pressure, a basalt of critical plane composition will fractionate to a syenitic liquid near the feldspar minimum, which is actually a narrow thermal maximum relative to the nepheline and silica minima. Morse suggested that a slight deviation from the critical plane composition should cause the liquid to migrate down one of the steep liquidus slopes to either side of this thermal maximum, producing phonolitic or rhyolitic residual liquids, respectively. However, Cox *et al.* (1979) argued that during fractionation of basalts lying slightly to either side of the thermal divide, the residual liquids are sufficiently enriched in alkalis to become trachytic long before the ultimate phonolitic or rhyolitic residues can be produced (Fig. 13). This appears to support the suggestion by Morse (1980) that the feldspar join of petrogeny's residual system may be more accurately represented by a thermal plateau than by a sharply defined saddle. It is also possible that the thermal maximum in this simple experimental system may disappear at high pressure or when additional components are added.

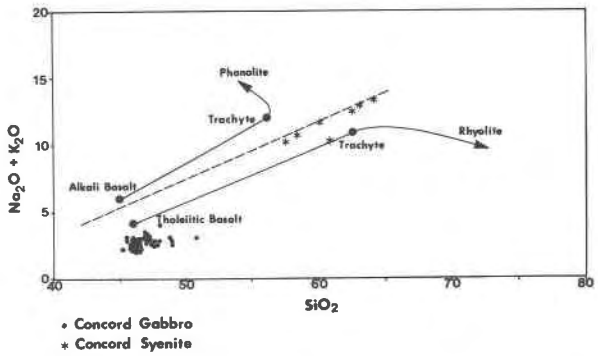

Fig. 13. Alkalis versus silica (wt.%) for Concord gabbro and syenite samples. The projection of the plane of critical silica undersaturation is represented by the dashed line (Ol–Cpx–Pl at the basaltic end, Ab–Or at the trachytic end, after Cox *et al.*, 1979). Basalts with compositions lying close to either side of this line (schematically represented by large dots) may fractionate to produce trachyte before "falling off" this thermal divide towards the phonolite or rhyolite minima.

The absence of any rocks of intermediate composition indicates that fractionation to form the syenitic liquid occurred at depth. Similar bimodal distributions are common in extrusive basalt–trachyte provinces (*e.g.*, Upton, 1974). One possible explanation for the missing intermediate rocks is that intermediate liquids may be more viscous, *i.e.*, less mobile, than basaltic and syenitic liquids (Upton, 1974). Another possibility is that a fairly flat portion of the liquidus trajectory between gabbro and syenite at high pressure might cause a large degree of fractionation over a small temperature interval, so that not many rocks of intermediate composition would be produced.

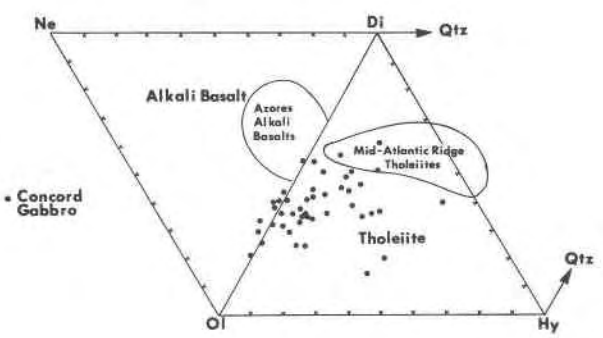

Fig. 12. Expanded normative basalt tetrahedron showing calculated values for analyzed Concord gabbros. Normative calculations are tabulated in Olsen (1982). Most compositions are tholeiitic, but many cluster about the Di–Ol join, the boundary between the tholeiitic and alkali basalt fields. Circled areas are compositional limits for flows (magma compositions) from typical basalt provinces.

Conclusions

(1) Geophysical modeling suggests the Concord complex consists of a 6 km-deep gabbro pluton surrounded by a steep-walled syenite ring dike, dipping outwardly at an angle of about 78° on the west side, with a vertical dip on the east side. This configuration probably resulted when the syenitic liquid intruded the fractured contact region between the gabbro body and the surrounding country rock.

(2) Gabbro and syenite crystallized nearly contemporaneously at 405 m.y. ago. Initial $^{87}Sr/^{86}Sr$ and $^{143}Nd/^{144}Nd$ ratios are consistent with the interpretation that both lithologies are related through igneous fractionation, and significant assimilation of crustal materials is excluded.

(3) Petrologic observations and geochemical modeling suggest that production of the Concord syenite involved extensive fractional crystallization of olivine, plagioclase,

and clinopyroxene, with minor oxide and sulfide minerals, from a basaltic parental magma similar in composition to the Concord gabbro. This fractionation occurred at depth before intrusion of the syenitic magma to the present level.

(4) The Concord trend probably reflects differentiation of a tholeiitic basaltic liquid to a syenitic residual liquid along a path near the critical plane of silica undersaturation. This trajectory may represent a thermal ridge of sufficient width to prevent fractionating melts from descending toward the rhyolite or phonolite minima before reaching syenitic compositions, or the thermal maximum in the analogous experimental system may have been modified by the effects of pressure or additional components.

Acknowledgments

We are grateful to the following individuals who have greatly aided this study: R. H. Hunter for assistance in geochemical modeling, K. C. Misra, L. A. Taylor, R. H. Hunter, J. R. Butler, and T. L. Wright for critical review; J. R. Butler for generously sharing chemical data; S. R. Hart for making facilities available for isotopic analyses; R. A. Hopkins for assistance with gravity modeling; and T. L. Grove for thoughtful discussion. Isotopic work was supported by NSF Grant EAR–7803342. Field work by the senior author was supported by grants from Sigma Xi and the Geological Sciences Professors' Honor Fund, University of Tennessee.

References

Albee, A. L. and Ray, L. (1970) Correction factors for electron probe microanalysis of silicates, oxides, carbonates, phosphates, and sulfates. Analytical Chemistry, 42, 1408–1414.

Amber, E. P. and Ashley, P. M. (1980) Mineralogy and petrology of the Dutchmans Creek gabbroic intrusion, South Carolina: discussion. American Mineralogist, 65, 1302–1303.

Arth, J. G. (1976) Behavior of trace elements during magmatic processes—a summary of theoretical models and their applications. U.S. Geological Survey Journal of Research, 4, 41–47.

Bell, H. (1960) A synthesis of geologic work in the Concord Area, North Carolina, U.S. Geological Survey Professional Paper 400B, 189–191.

Bence, A. E. and Albee, A. L. (1968) Empirical correction factors for the electron microanalysis of silicates and oxides. Journal of Geology, 76, 382–403.

Butler, J. R. and Ragland, P. C. (1969) A petrochemical survey of plutonic intrusions in the Piedmont, Southeastern Appalachians, U.S.A. Contributions to Mineralogy and Petrology, 24, 164–190.

Cabaup, J. (1969) Origin and differentiation of the gabbro in the Concord ring dike, North Carolina Piedmont. Unpublished M.S. Thesis, University of North Carolina at Chapel Hill.

Cox, K. G., Bell, J. D. and Pankhurst, R. J. (1970) The Interpretation of Igneous Rocks. Allen and Unwin, London.

Fullagar, P. D. (1971) Age and origin of plutonic intrusions in the Piedmont of the southeastern Appalachians. Geological Society of America Bulletin, 82, 2845–2862.

Fullagar, P. D. and Butler, J. R. (1979) 320 to 260 Myr-old post-metamorphic granitic plutons in the Piedmont of the southeastern Appalachians. American Journal of Science, 279, 161–185.

Gast, P. W. (1968) Trace element fractionation and the origin of tholeiitic and alkaline magma types. Geochimica et Cosmochimica Acta, 32, 1057–1086.

Greenland, L. P. (1970) An equation for trace-element distribution during magmatic crystallization. American Mineralogist, 55, 455–465.

Irvine, T. N. (1982) Terminology for layered intrusions. Journal of Petrology, 23, 127–162.

Johnson, R. W. and Bates, R. G. (1960) Aeromagnetic and aeroradioactivity survey of the Concord Quadrangle, North Carolina. U.S. Geological Survey Professional Paper 400B, 182–195.

Jones, L. M. and Walker, R. L. (1973) Rb–Sr whole rock age of the Siloam granite, Georgia: A Permian intrusive in the southern Appalachians. Geological Society of America Bulletin, 84, 3653–3658.

Leake, B. E. (1978) Nomenclature of amphiboles. American Mineralogist, 63, 1023–1052.

LeGrand, H. E. and Mundorff, M. J. (1952) Geology and ground water in the Charlotte area, North Carolina. North Carolina Department of Conservation and Development, Bulletin 63.

McCallum, I. S., Raedeke, L. D. and Mathez, E. A. (1980) Investigations of the Stillwater complex: Part I: stratigraphy and structure of the banded zone. Americal Journal of Science, 280A, 59–87.

McSween, H. Y. (1980) Mineralogy and petrology of the Dutchmans Creek gabbroic intrusion, South Carolina: reply. American Mineralogist, 65, 1304–1306.

Medlin, J. H. (1968) Comparative petrology of two igneous complexes in the South Carolina Piedmont. Unpublished Ph.D. Thesis, Pennsylvania State University.

Morgan, B. A. and Mann, V. I. (1964) Gravity studies in the Concord Quadrangle, North Carolina. Southeastern Geology, 5, 143–155.

Morse, S. A. (1980) Basalts and Phase Diagrams. Springer–Verlag, New York.

Neilson, M. J. and Brockman, G. F. (1977) The error associated with point counting. American Mineralogist, 62, 1238–1244.

Nockolds, S. R. (1954) Average chemical compositions of some igneous rocks. Geological Society of America Bulletin, 65, 1007–1932.

Olsen, B. A. (1982) Petrogenesis of the Concord gabbro–syenite complex, Cabarrus County, North Carolina. Unpublished M.S. Thesis, University of Tennessee at Knoxville.

Pearce, J. A. and Norry, M. J. (1979) Petrogenetic implications of Ti, Zr, Y, and Nb variations in volcanic rocks. Contributions to Mineralogy and Petrology, 69, 33–47.

Price, V. (1969) Distribution of trace elements in plutonic rocks of the southeastern Piedmont. Unpublished Ph.D. Thesis, University of North Carolina at Chapel Hill.

Sando, T. W. and Hart, S. R. (1982) Nd isotope geochemistry of Hercynian granitic rocks of the southeastern Appalachians. Geological Society of America abstracts with programs, 14, 79.

Sneeringer, M. A. (1981) Strontium and samarium diffusion in diopside. Unpublished Ph.D. Thesis, Massachusetts Institute of Technology.

Streckeisen, A. L. (1973) Plutonic rocks—classification and nomenclature. Geotimes, 18, 43–63.

Talwani, M., Worzel, J. L. and Landisman, M. (1959) Rapid gravity computations for two-dimensional bodies with application to the Mendocino submarine fracture zone. Journal of

Geophysical Research, 64, 49–59.

Upton, B. G. J. (1974) The alkaline province of south–west Greenland. In H. Sorensen, Ed., The Alkaline Rocks, p. 221–238, Wiley and Sons, London.

Van der Plas, L. and Tobi, A. C. (1965) A chart for judging the reliability of point counting results. American Journal of Science, 263, 87–90.

Watson, T. L. and Laney, F. B. (1906) The building and ornamental stones of North Carolina. North Carolina Geological Survey Bulletin, 2.

White, W. A. and Mundorff, M. J. (1944) Unpublished geologic map of the Concord area, North Carolina.

Wilson, F. A. (1981) Geologic interpretation of geophysical data from the "Mecklenburg–Weddington" gabbro complex, southern Mecklenburg County, North Carolina. In J. W. Horton, J., J. R. Butler and D. M. Milton, Eds., Geological Investigations of the Kings Mountain Belt and Adjacent Areas in the Carolinas, p. 28–37, Carolina Geological Society Field Trip Guidebook, S. C. Geological Survey, Columbia.

Wright, T. L. and Doherty, P. C., (1970) A linear programming and least squares computer method for solving petrologic mixing problems. Geological Society of American Bulletin, 81, 1995–2008.

York, D. (1966) Least–squares fitting of a straight line. Canadian Journal of Physics, 44, 1079–1086.

Zindler, A., Hart, S. R., Frey, F. A. and Jakobsson, S. P. (1979) Nd and Sr isotope ratios and rare-earth element abundances in Reykjanes Peninsular basalts: evidence for mantle heterogeneity beneath Iceland. Earth and Planetary Science Letters, 45, 249–262.

Manuscript received, March 16, 1982;
accepted for publication, October 13, 1982.